Short-Beam and Three-Point-Bending Tests for the Study of Shear and Flexural Properties in Unidirectional-Fiber-Reinforced Epoxy Composites

E. Sideridis, G. A. Papadopoulos

Department of Engineering Science, Section of Mechanics, National Technical University of Athens, 5 Heroes of Polytechniou Avenue, GR-15773 Zographou, Athens, Greece

Received 18 June 2003; accepted 19 December 2003
DOI 10.1002/app.20382
Published online in Wiley InterScience (www.interscience.wiley.com).

ABSTRACT: The bending properties of composite materials are often characterized with simply supported beams under concentrated loads. The results from such tests are commonly based on homogeneous beam equations. For laminated materials, however, these formulas must be modified to account for the stacking sequence of the individual plies. The horizontal shear test with a short-beam specimen in three-point bending appears suitable as a general method of evaluation for the shear properties in fiber-reinforced composites because of its simplicity. In the experimental part of this work, the shear strength of unidirectional-glass-fiber-reinforced epoxy resin composites was determined in different fiber directions with the short-beam three-point-bending test. Also, the elastic constants and flexural properties of the same materials were determined from bending experiments carried out on specimens in the 0, 15, 30, 45, 60, 75, and 90° fiber directions with high span–thickness ratios. © 2004 Wiley Periodicals, Inc. J Appl Polym Sci 93: 63–74, 2004

Key words: unidirectional-fiber-reinforced epoxy composite; short-beam test; three-point bending test; elastic constants

INTRODUCTION

Knowledge of the shear properties is very important whenever the interfacial bonding or matrix failure of a composite material is critical, such as in a composite structure subjected to compression loading. However, because so many methods have been developed to measure shear, there is a great deal of confusion about which shear method should be used. Ideally, a test method should produce pure shear. However, this is difficult to attain because of coupling effects. In addition to producing pure shear, a good shear test method should give reproducible results, provide all shear properties, require no special equipment for specimen preparation, be capable of being performed on readily available testing machines, and have a simple data reduction procedure.

Numerous methods are available for measuring shear properties.[1] Among them, the torsional shear of a thin, walled tube, the torsional shear of a unidirectional composite rod, the tensile shear of ±45° off-axis laminates, the tensile shear of 10° off-axis laminates, the interlaminar tensile shear of a grooved laminate, and the interlaminar shear of a short beam are used mostly.

Correspondence to: E. Sideridis.

Journal of Applied Polymer Science, Vol. 93, 63–74 (2004)

The short-beam shear test has become a widely used method for characterizing the interlaminar failure resistance of fiber-reinforced composites. This test method involves loading a beam under three-point bending (see Fig. 1) with certain dimensions so that interlaminar shear failure is induced.

The simplicity of the test method makes it a very popular screening tool. The experimental requirements for such a test on a fiber-reinforced composite are simpler than those for a tensile test because the effects of flaws and geometrical stress concentrations are less severe. In addition, a rectangular cross-sectional specimen can be used, and this leads to ease of sample preparation. Also, there is no need to provide end tabs on a reduced cross section to ensure failure away from the grips.[2]

In a general review of material evaluation bending tests, Mullin and Knoell[3] discussed the theoretical origins of L/t ratios (where L is the span length and t is the nominal thickness) and the effects of material variables and specimen defects such as voids, and Westwater[4] observed that specimens with small L/t ratios often fail by cracks running out to, or past, the support nose and also that the amount of overhang may affect the mode of failure. Daniels et al.[5] demonstrated representative failure modes of carbon-fiber/epoxy-resin composites in short-beam tests but indicated that the same behavior would not necessarily occur for other combinations of materials. Whitney and Browning[6] referred to the limitations of the short-beam shear method.

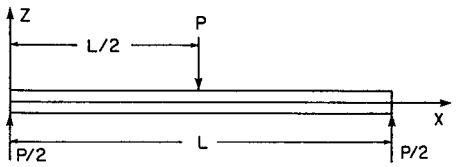

Figure 1 Three-point-bending test.

The applicability of the short-beam shear test has been questioned by other researchers. Berg et al.[7] used an elastoplastic finite-element code to perform a stress analysis on an orthotropic short-beam shear specimen. Sandorff[8] studied the effect of stress concentrations on the elastic response of orthotropic beams. His results showed that the short-beam shear configuration yields stress-concentration effects that are never fully dissipated, as St. Venant's principle is not satisfied in a highly orthotropic beam of a low span-to-depth ratio.

In this article, we present the results of a experimental study for the evaluation of the interlaminar shear strength of epoxy-resin/glass-fiber composites with fiber directions ranging from 0 to 90° according to ASTM D 2344.[9] Also, the elastic constants and flexural properties of the same material were determined from bending experiments carried out on specimens with large L/t ratios.

ANALYSIS

At small L/t ratios, an orthotropic beam of low shear strength is expected to fail by shear at the neutral axis. At progressively larger L/t ratios, the mode of failure becomes flexural. In this situation, the outer fibers fail in tension if, as is usual, the tensile strength is less than the compressive strength. There is an intermediate range of L/t ratios in which the behavior is transitional, and the mode of failure may vary from sample to sample or assume aspects of both modes as deformation proceeds. As shown in Figure 1, which illustrates the mechanics of the test method, the specimen is supported by the reaction noses and the load is applied at a constant speed through the loading nose. The stress at any point in the beam can be calculated to a first approximation with mechanics-of-materials theory. This theory is based on the necessary conditions for static equilibrium, which pertains here because the rate of deformation is small.

The basic assumptions of the theory are as follows:

1. The external forces are applied at thin lines and not distributed over finite areas.
2. $\varepsilon_x \propto y$ (ε_x is the axial strain and y the vertical to the plane xz axis).
3. $\sigma_y = \sigma_z = 0$ (σ_y and σ_z are the transverse normal stresses).
4. $\sigma_x = E\varepsilon_x$ (where σ_x is the longitudianl normal stress and E the elastic modulus).
5. τ_{xz} is independent of y (where τ_{xz} is the interlaminar shear stress).
6. $\tau_{xy} = 0$ (τ_{xy} is the in-plane shear stress).

After the equilibrium conditions are applied for stresses σ_x and τ_{xz}, these two major components of the stress can be obtained. σ_x has its maximum tensile or compressive value at the lower or upper point of the specimen:

$$\sigma_x = \frac{3PL}{2bt^2} \tag{1}$$

τ_{xz}, which is maximum at the neutral axis, is given by

$$\tau_{xz} = \frac{3P}{4bt} \tag{2}$$

where P is the load and b is the width of the specimen.

Because the theory involves many approximations, S_H is used to denote the apparent short-beam shear strength given by eq. (2). The two stresses are related:

$$\frac{\sigma_x}{\tau_{xz}} = \frac{2L}{t} \tag{3}$$

When the shear stress is constant, the flexure stress varies linearly with L/t, and when the flexure stress is constant, the shear stress varies as an hyperbolic function of L/t.

If in an experiment the shear stress at failure is τ_F and the flexure stress (tensile or compressive stress) at the same load is σ_F, eq. (3) can be rewritten as

$$\frac{\sigma_F}{\tau_F} = \frac{2L}{t} \tag{4}$$

if elastic behavior is assumed.

If the failure stress in shear is τ_M (the maximum shear stress) and the failure stress in flexure is σ_M (the maximum flexural stress), the failure of the specimen in shear occurs when

$$\tau_F = \tau_M \quad \text{and} \quad \sigma_F < \sigma_M \tag{5}$$

From eq. (4), we have

$$\frac{\tau_F}{\sigma_F} > \frac{\tau_M}{\sigma_M} \quad \text{or} \quad \frac{\tau_M}{\sigma_M} < \frac{t}{2L} \tag{6}$$

If the failure of the specimen is in flexure, then

$$\sigma_F = \sigma_M \quad \text{and} \quad \tau_F < \tau_M \tag{7}$$

From eq. (4), we have

$$\frac{\tau_F}{\sigma_F} < \frac{\tau_M}{\sigma_M} \quad \text{or} \quad \frac{\tau_M}{\sigma_M} > \frac{t}{2L} \tag{8}$$

If we assume that for a material the ratio of σ_M to τ_M is constant, that is,

$$\frac{\sigma_M}{\tau_M} = C \tag{9}$$

the beam will fail in shear rather than in flexural tension in compression if

$$C > \frac{2L}{t} \tag{10}$$

Therefore, C can be theoretically estimated by the calculation of the parameter $2(L/t)$ for a composite and by the observation of the types of failure occurring. For shear failure (debonding at the middle of the thickness), this ratio should be below the value of C, and for flexural (surface) failure, it should be above the value of C. However, the composite strength for a fiber angle (θ) of 0° can be calculated with the rule of mixtures:

$$\sigma_c = \sigma_f \upsilon_f + \sigma'_m(1 - \upsilon_f) \tag{11}$$

where σ_c and σ'_f denote the failure stresses of the composite and fibers, respectively; σ'_m is the matrix stress when the fiber failure strain is reached; and υ_f is the fiber content.

According to the Bernouilly–Euler theory, the elastic deflection arising from a flexural stress in a rectangular beam (δ_B) is (Fig. 1)

$$\delta_B = \frac{PL^3}{48E_xI_y}\left(\frac{x}{L}\right)\left(3 - 4\,\frac{x^2}{L^2}\right) \quad 0 \le x \le L/2 \tag{12}$$

where I_y denotes the moment of inertia of the section.

The elastic shear deflection (δ_s) in the same beam is

$$\delta_s = \frac{\mu Px}{2G_{xz}A} \quad 0 \le x < \frac{L}{2} \tag{13}$$

where G_{xz} is the interlaminar shear modulus, A is the area of the section, and μ is its shape factor (6/5 for this case). The total deflection (δ_t) is the sum of these two components:

$$\delta_t = \delta_B + \delta_s = \frac{PL^3}{48E_xI_y}\left(\frac{x}{L}\right)\left(3 - 4\,\frac{x^2}{L^2}\right) + \frac{\mu Px}{2G_{xz}A} \tag{14}$$

Thus, the deflection at midpoint M (δ_M), given that $A = bt$ and $I_y = (bt^3)/12$, is

$$\delta_M = \delta_{\max} = \frac{PL^3}{48E_xI_y}\left(1 + \frac{12\mu EI_y}{G_{xz}AL^2}\right) = \frac{PL^3}{48E_xI_y}\left[1 + \frac{6}{5}\left(\frac{E_x}{G_{xz}}\right)\left(\frac{t}{L}\right)^2\right] \tag{15}$$

The ratio of the two deflections is

$$\frac{\delta_s}{\delta_B} = \frac{6}{5}\left(\frac{E_x}{G_{xz}}\right)\left(\frac{t}{L}\right)^2 \tag{16}$$

G_{xz} can be evaluated from eq. (15) as follows:

$$G_{xz} = \frac{3PL}{10bt\left(\delta_{\max} - \dfrac{PL^3}{48E_xI_y}\right)} \tag{17}$$

EXPERIMENTAL

The unidirectional-glass-fiber composite used in this study consisted of long E-glass fibers (Permaglass XE B5/1) embedded in an Araldite MY 750 HT 972 epoxy resin based on diglycidyl ether of bisphenol A together with an aromatic amine hardener. The glass fibers had a diameter of 12×10^{-6} m and were contained in a volume fraction of $\upsilon_f = 0.65$.

υ_f was determined, as customary, through the ignition of samples of the composite and the weighing of the residue; this gave the weight fraction of glass as $m_f = 79.6 \pm 0.28\%$. This and the measured values of the relative densities of the glass ($\rho_f = 2.55$) and epoxy resin ($\rho_m = 1.20$) gave the υ_f value of 0.65.

Rectangular specimens, for which ℓ was 7 cm and b was 1.5 cm with $L = 3.2$ cm and $t = 0.60$ cm (varying from 0.55 to 0.65 cm), were used during the short-beam-bending experiments according to ASTM D 2344. However, for the determination of the elastic constants, rectangular specimens, for which ℓ was 20 cm and b was 2 cm with $L = 10$ cm and $t = 0.60$ cm, were used during three-point-bending experiments according to ASTM D 790. Two Kyowa KFP-2C1-65 strain gauges (horizontal and perpendicular) with a gauge length of 2 mm and a gauge factor of 1.99 were put on the specimens to determine the strains. Four specimens for each of the fiber directions (0, 15, 30, 45, 60, 75, and 90°) were used during the experiments, which were carried out at 0.2 cm/min for all cases on an Instron testing machine.

TABLE I
Experimental Values for σ_F and τ_F for $L/t = 5$

	Θ (°)	t (mm)	b (cm)	P_F (N)	σ_F (MPa)	$\bar{\sigma}_F$ (MPa)	τ_F (MPa)	$\bar{\tau}_F$ (MPa)
1	0	5.8	1.55	6200	570.75	541.42	51.72	49.06
2		5.8	1.55	6001	552.34		50.06	
3		5.8	1.55	6550	525.06		47.58	
4		5.8	1.55	6420	517.54		46.92	
5	15	5.8	1.54	5270	488.29	500.91	44.25	44.09
6		5.6	1.53	5180	514.84		45.34	
7		5.6	1.53	4940	494.19		43.24	
8		5.5	1.52	4850	506.31		43.51	
9	30	5.9	1.54	3020	270.41	279.63	24.93	25.35
10		5.8	1.54	3110	288.15		26.11	
11		5.7	1.56	2720	257.59		22.94	
12		5.8	1.51	3200	302.38		27.41	
13	45	6.1	1.55	1440	119.84	129.46	11.42	12.49
14		6.2	1.55	1790	144.21		13.97	
15		6.2	1.41	1310	116.01		11.24	
16		6.2	1.45	1600	137.79		13.35	
17	60	6.2	1.54	1070	86.76	94.44	8.41	9.11
18		6.2	1.53	1070	87.33		8.46	
19		6.2	1.52	1180	96.94		9.32	
20		6.3	1.53	1350	106.71		10.51	
21	75	6.2	1.55	1020	82.17	79.89	7.96	7.67
22		5.9	1.56	1000	88.39		8.15	
23		6.4	1.56	920	69.11		6.91	
24		6.2	1.54	660	—		—	
25	90	5.8	1.68	930	78.98	71.14	73.89	6.65
26		6.0	1.56	750	64.10		60.10	
27		6.1	1.58	820	66.95		63.81	
28		5.8	1.49	780	74.69		67.69	

RESULTS AND DISCUSSION

Table I contains the mean experimental values for the load (P_F), the normal stress (σ_F), and shear stress (τ_F) at failure of the composite material for θ tested in three-point bending for $L/t = 5$. The same results for $L/t = 5$ and $L/t = 16$ are illustrated in Figures 2 and 3, respectively, versus θ of the composite. Both the normal and shear stress show abrupt decreases up to 45°, and then up to 90° the decreases become smooth. Also, although for $L/t = 16$ the normal stress values (σ) are greater than the respective values for $L/t = 5$, in the case of the shear stress (τ), there is an opposite effect; that is, the values for $L/t = 5$ are greater than those for $L/t = 16$. This means that the apparent shear strength depends strongly on the L/t ratio.

Figures 4 and 5 illustrate the boundary of shear and tensile (or compressive) flexural failures for $L/t = 5$ and $L/t = 16$, respectively, as denoted in eqs. (9) and (10), which are derived from the theory. In each figure, the straight line represents the boundary between shear and tensile flexural failures according to inequality (10). The experimental data show good agreement with the theory in both cases because the shear failures occurring for $L/t = 5$ lie above the straight line (Fig. 4), whereas the tensile flexural failures occurring for $L/t = 16$ lie below this line (Fig. 5). From this, it can be concluded that the shear strength depends strongly on the L/t ratio even for shear failures. This effect could be due to local stress concentrations (at the ends of the specimen and at the noses), which are ignored in the elementary theory. Alternatively, it could be a combined stress effect. If the shear strength were enhanced by the presence of a transverse compressive stress, then an increased value of S_H at the smallest value of L/t would be expected. The shear

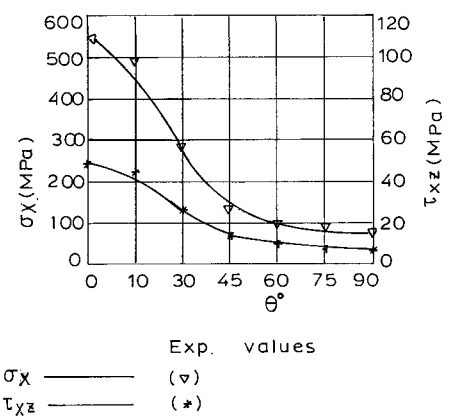

Figure 2 Variation of σ_x and τ_{xz} versus θ for $L/t = 5$.

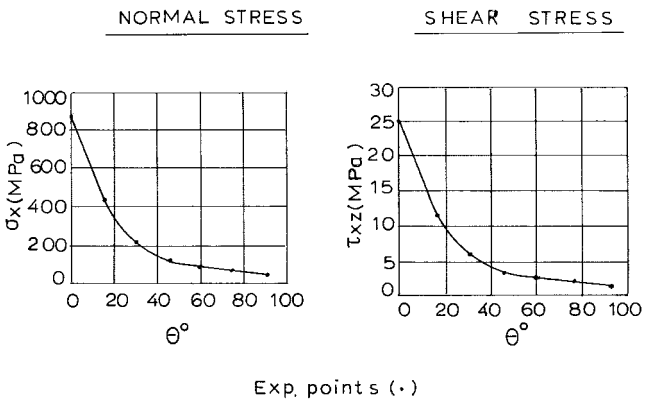

Figure 3 Variation of σ_x and τ_{xz} versus θ for $L/t = 16$.

failures in the specimens tested occurred with the plane of shear near the neutral axis, that is, at $t/2$, and exceptions to this may be due to the specimen preparation procedure, which can leave resin-rich areas.

The interlaminar shear strength depends on the fiber direction, and it decreases as θ varies from 0 to 90°. On the contrary, it is expected to be essentially independent of the fiber volume fraction; this indicates that, at the plane of shear, the existence of proportionately more fibers nearby does not affect the strength for shear failure.

It is evident from eq. (4) that when the shear stress (τ) is a constant, the flexure stress will vary linearly with L/t, and when the flexure stress is a constant, the interlaminar shear stress will vary as a hyperbolic function of L/t.

To evaluate the composite flexure strength for $\theta = 0$, let us consider eq. (11) and Figure 6. With values of $\sigma_f = 1250$ MN/m^2 and $\varepsilon_f = 17 \times 10^{-3}$ for the failure stress and strain of the glass fibers and $\sigma'_m = 56$ MN/m^2 for the epoxy resin stress when fiber

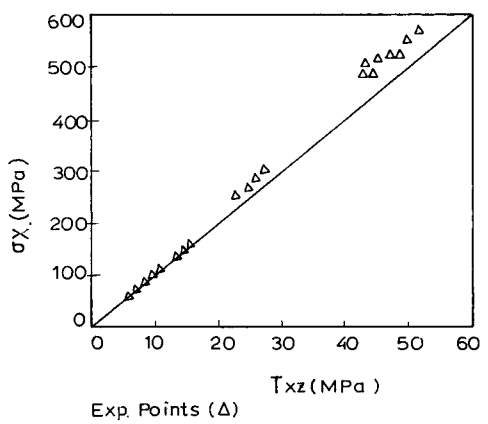

Figure 4 Boundary of shear and tensile (or compressive) flexural failure for $L/t = 5$.

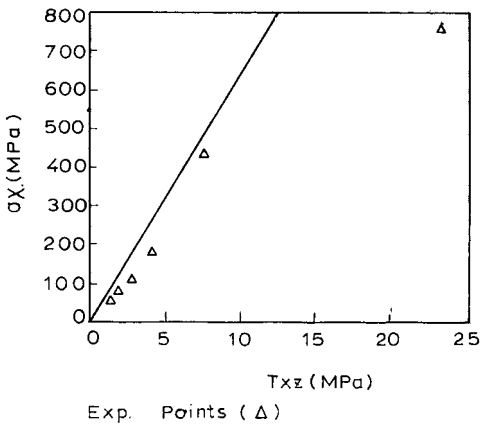

Figure 5 Boundary of shear and tensile (or compressive) flexural failure for $L/t = 16$.

failure strain is reached, the value of $\sigma_c = 832.1$ MN/m^2 can be obtained for the composite strength for $v_f = 0.65$. This shows some discrepancy with the respective mean experimental value appearing in Table II.

A factor producing confusion in the interpretation of the results is that, with this high fiber volume fraction $v_f = 0.65$ and $L/t = 5$, indentation by the central loading nose caused compressive failure

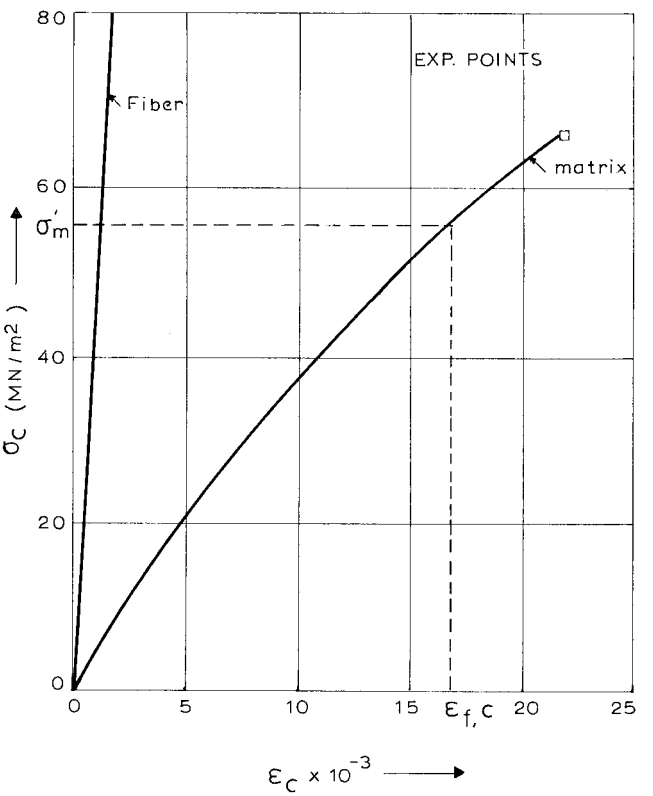

Figure 6 Stress–strain diagram for the fiber and matrix material.

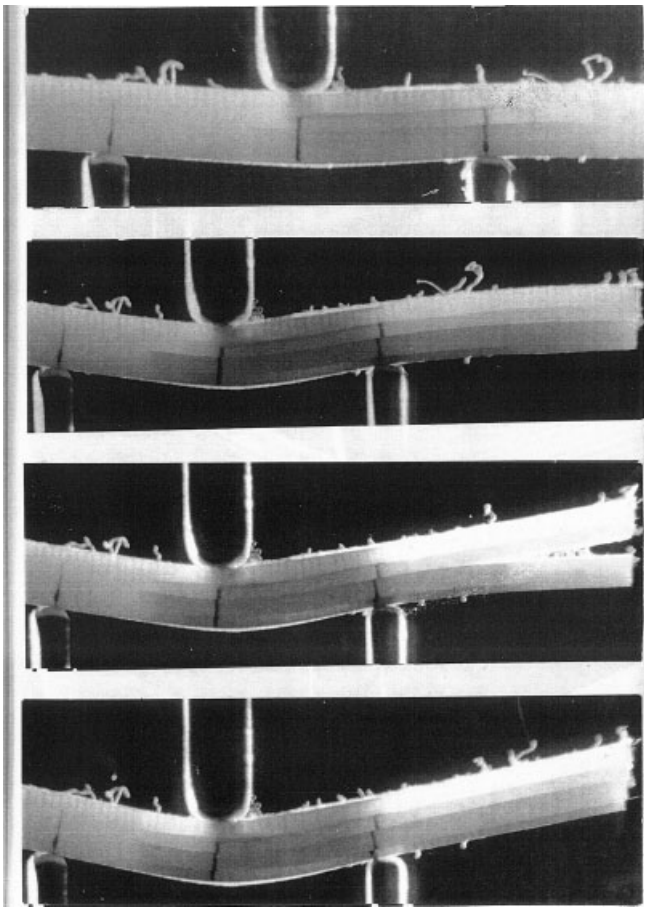

Figure 7 Example of the shear failure mode.

zone. This preceded shear failure and, in some cases, appeared to initiate shear failure, as shown in Figure 7.

Figure 8 illustrates P–δ diagrams for various θ values (0–90°) obtained from short-beam three-point-bending experiments, that is, for $L/t = 5$. There is a large decrease in the failure load (or failure moment) when θ increases from 0 to 90°, and the deflection at fracture decreases as expected. However, if we look carefully, we can see that the slope of the curves in these diagrams does not show large discrepancies. That is, there is not a significant difference in the variation of δ versus θ. There is a maximum at $\theta = 45°$.

Figure 9 presents P–δ diagrams for θ values varying from 0 to 90°, as obtained from three-point-bending experiments for $L/t = 16$. The values of δ are much higher than the respective ones for $L/t = 5$, and for the two types of bending, the concave and convex sides of the respective P–δ curves are opposite.

Figure 10 presents P–ε diagrams for various θ values (0–90°), as obtained from three-point-bending experiments for $L/t = 16$. The P–ε curves have a more linear behavior at low and high θ values and show a maximum curvature for $\theta = 45°$.

From these diagrams, the experimental values for the elastic modulus (E_x) and Poisson ratio (ν_{xy}) for various values of θ can be obtained. These values appear in Figure 11. As expected, E_x decreases as θ increases from 0 to 90°. However, there is a slight increase for $\theta = 60°$ and $\theta = 75°$ and then a slight decrease, after which E_x is almost the same for $\theta = 90°$ and for $\theta = 45°$. Also, $E_x = 41.02$ GPa for $\theta = 0°$ seems much lower than expected, and this can be verified through the calculation of the elastic modulus by the mixture law formula, $E_L = E_f v_f + E_m(1–v_f)$, where E_L is the longitudinal modulus. For the composite material used, the elastic moduli for the fiber and matrix are $E_f = 72$ GPa and $E_m = 3.5$ GPa, respectively, and v_f is 0.65 as previously mentioned. This formula yields the value $E_L = 48.03$ GPa, which is much higher than the experimental one.

The values of ν_{xy} follow the expected behavior. They increase when θ increases, they obtain a maximum, and then they decrease again as θ goes to 90°. The experimental value of ν_{xy} for $\theta = 0°$ does not seem to be significantly different from what was expected, and this can be verified by the calculation of the longitudinal Poisson ratio (ν_{LT}) with the mixture law formula: $\nu_{LT} = \nu_f v_f + \nu_m v_m$. For the composite, the Poisson ratios for the fiber and matrix are $\nu_f = 0.20$ and $\nu_m = 0.36$, respectively. For $v_f = 0.65$, this formula yields $\nu_{LT} = 0.255$, which is slightly higher than the experimental value. The low value of E_x for $\theta = 0°$ leads to the nonvalidity of the Maxwell law, that is, $E_L/\nu_{LT} = E_T/\nu_{TL}$ [where $E_L = (E_x)_{\theta=0°}$, $E_T = (E_x)_{\theta=90°}$, $\nu_{LT} = (\nu_{xy})_{\theta=0°}$, and $\nu_{TL} = (\nu_{xy})_{\theta=90°}$], which shows a large discrepancy.

This fact led us to investigate the likelihood of an error due to the misalignment of the strain gauges or to the cutting of the specimen. Thus, if it is assumed that there is such an error of $\beta = 5°$, the strains will be calculated with eq. (A.1) as follows.

From Figure 10, for $\theta = 0°$ and for $P = 250$ N, $\varepsilon_x = 2351 \times 10^{-6}$, $\varepsilon_y = -587 \times 10^{-6}$, and $\gamma_{xy} = 0$, we obtain $\varepsilon'_x = 2329 \times 10^{-6}$ and $\varepsilon'_y = 565 \times 10^{-6}$, which, by the use of eq. (A.1) and the definitions of E_x and ν_{xy}, yield $E_x = 41.4$ GPa and $\nu_{xy} = 0.243$, which are not too much different from the previous experimental values. This shows that the discrepancy is not due to the assumed error. It may instead be due to the influence of a possible resin-rich layer in the composite, which is more important in the case of bending than in the case of tension, but is mainly due to the variation of the bending modulus (E_b) with L/t, which tends asymptotically to the value of E_x obtained in tension for very large values of L/t (e.g., $L/t > 60$, as stated in ref. 10).

Indeed, as stated in the appendix, if it is assumed that a resin-rich layer exists on either or both surfaces

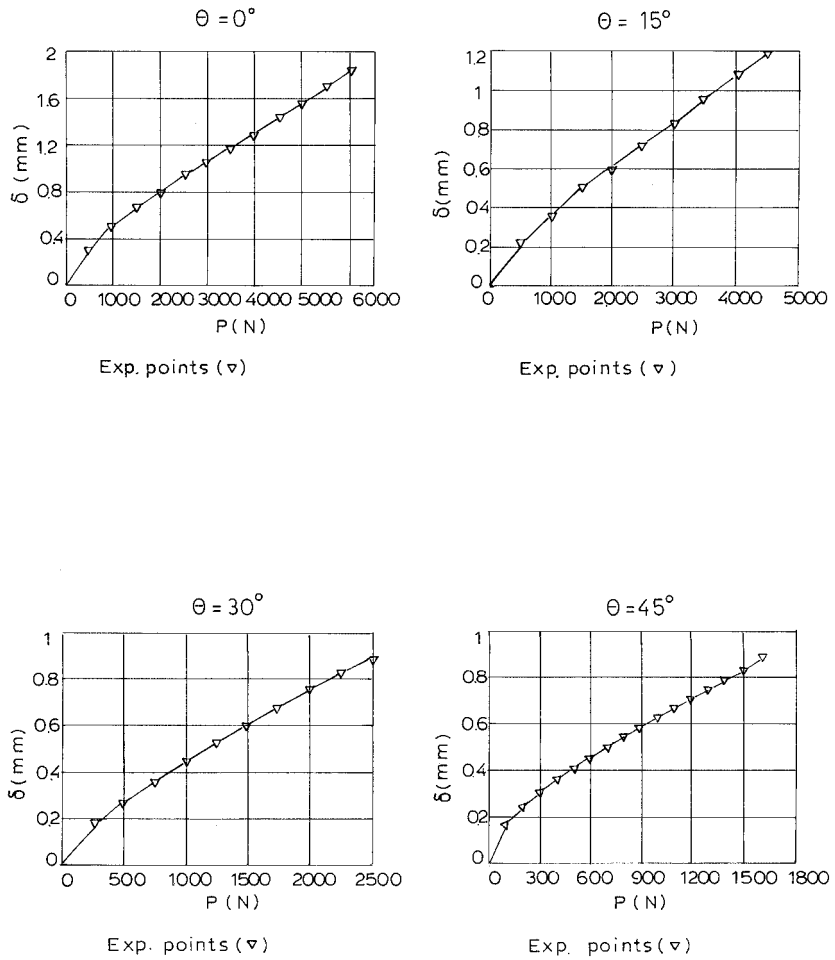

Figure 8 P–δ diagrams for various values of θ for $L/t = 5$.

of a composite of thickness $t_{RRL} = \Delta t = 0.25$ mm, in the total mean thickness of 6 mm of the specimens used during the experiments, with eqs. (A.2), (A.5), and (A.6) and with the previously calculated theoretical value $E_L = 48.03$ GPa, the moduli $E_t' = 46$ GPa and $E_b' = 42$ GPa can be obtained. This shows how such a resin-rich layer influences E_b.

To verify the effect of L/t on the discrepancy between the longitudinal values of E_b and the extensional modulus (E_t), we carried out a tensile experiment on a similar specimen with $\theta = 0°$, $L = 25$ cm, $b = 1.9$ cm, and $t = 6.1$ mm. From the diagram of Figure 12, E_L was calculated to be 48.20 GPa, a value in very good agreement with the theoretical value found previously. The experimental value of ν_{LT}, 0.252, is too close to the respective experimental value obtained from bending experiments, which already was in good agreement with the theoretical value. Thus, it can be expected that with increasing L/t, E_b will approach the tensile modulus, as stated in ref. 10.

E_b was also estimated from the deflection with eq. (12) and the P–δ diagrams for various θ values in Figure 9. The results are presented in Figure 13. These results show some discrepancy for $\theta = 0°$ and $\theta = 90°$ in comparison with those derived from bending experiments with strain-gauge measurements. In particular, the value of E_x for $\theta = 0°$, which is around 38 GPa, shows a large discrepancy in comparison with the respective theoretical value and that derived from the tensile experiment. The value for $\theta = 90°$, which is around 16 GPa, seems more realistic because the E_x curve does not present a slight increase for this angle as the E_x curve does that was derived from strain-gauge measurements.

To determine the cause of this discrepancy, let us consider eqs. (15) and (16). It is obvious that because the G_{xz}/E_x ratio is much lower for composites than for metals, the shear deformation is more significant in these materials, especially when L/t is low, as can be observed from eq. (16). Thus, δ_s has a larger

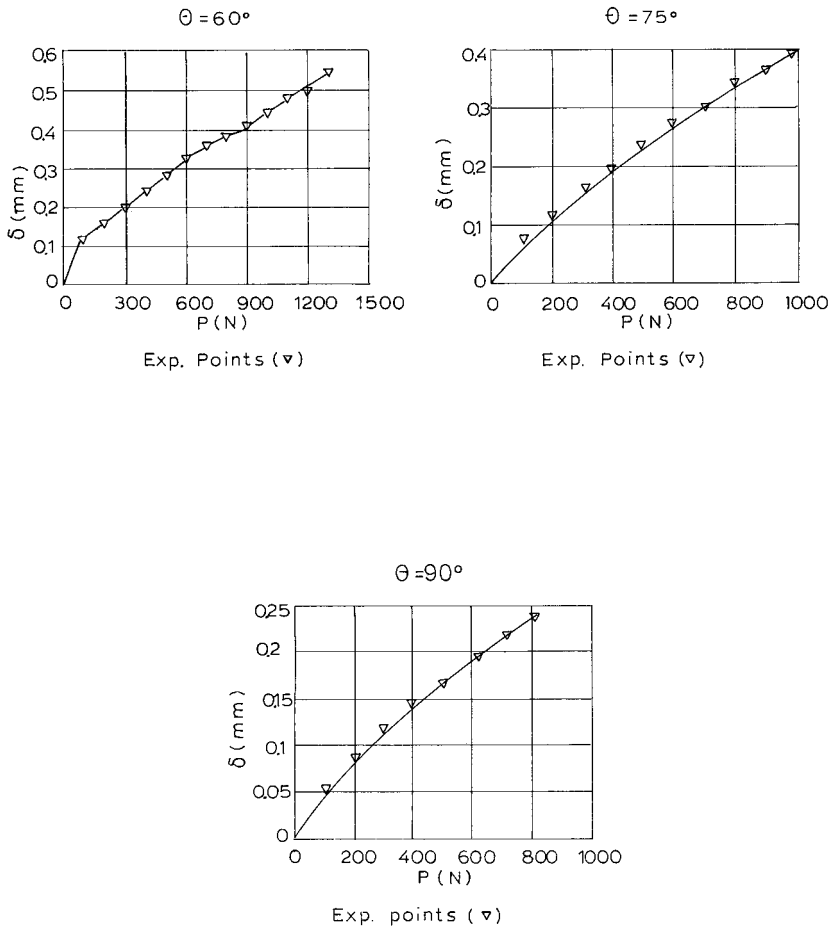

Figure 8 (*Continued from the previous page*)

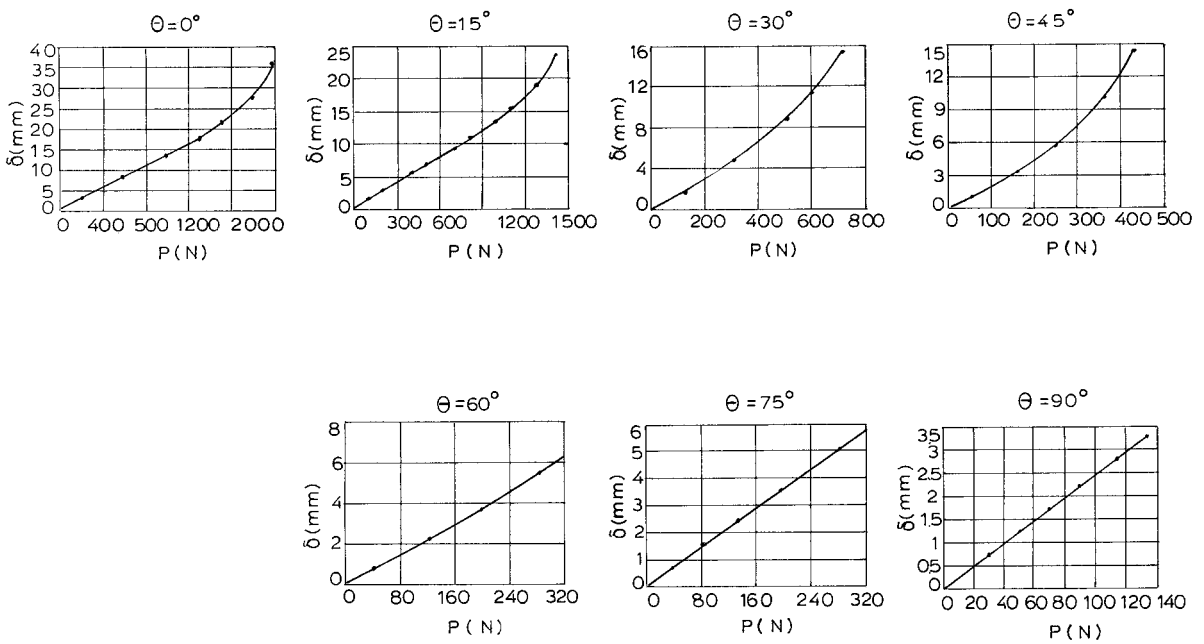

Figure 9 P–δ diagrams for various values of θ for $L/t = 16$.

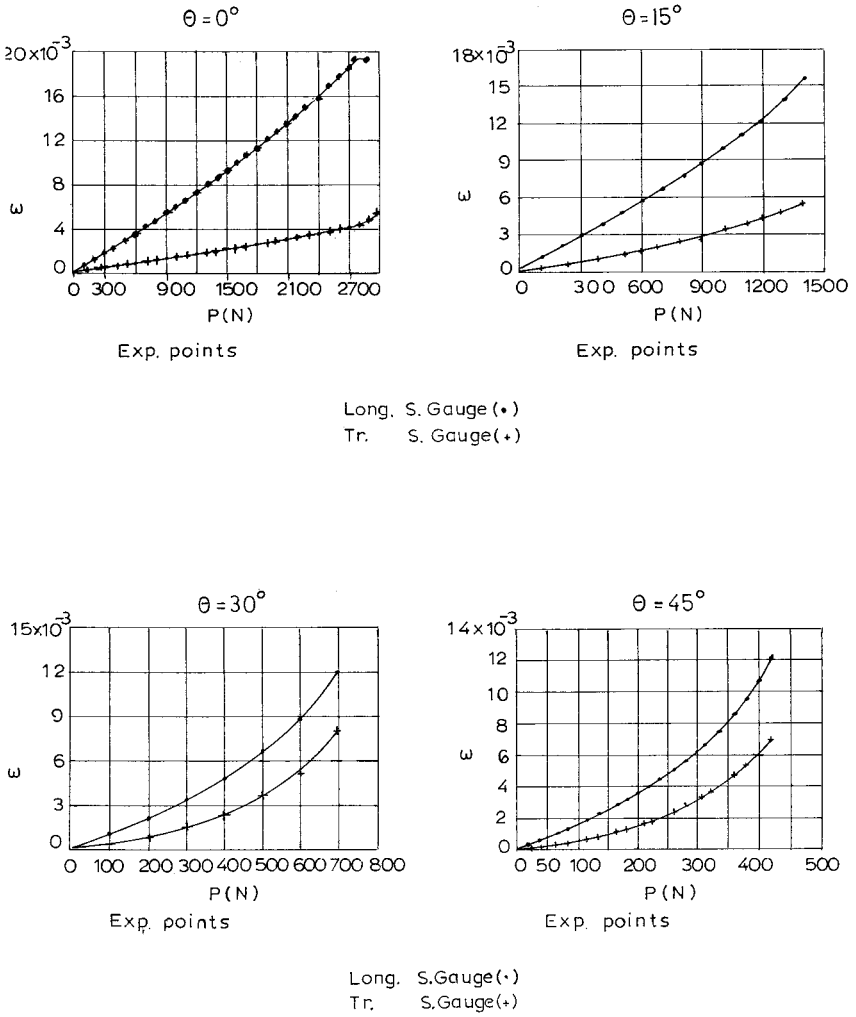

Figure 10 P–ε diagrams for various values of θ for $L/t = 16$.

contribution to δ_t when E_x/G_{xz} and t/L are high, as can be observed from eq. (15). For L/t ratios of 5, 16, 32, and 40, the contribution becomes $0.048(E_x/G_{xz})$, $0.0047(E_x/G_{xz})$, $0.0012(E_x/G_{xz})$, and $0.0008(E_x/G_{xz})$, respectively; that is, there is an increase of 10, 40, or 60 times, respectively. Because E_x for $\theta = 0°$ has a large value, the ratio of the two moduli is high, and the contribution of the last term in eq. (15) is more important. This explains the fact that E_x shows a large discrepancy for $\theta = 0°$ when evaluated from the deflection. It can be concluded that for the apparent value of E_b, which can be found under the assumption that δ_t is due mainly to bending, to be as nearly equal to the true value of E_b as possible, δ_s must be very low ($\delta_s/\delta_B \ll 1$).

G_{xz}, calculated from eq. (17) with the values given in Figure 8 and with the specimen characteristics, is 0.35 GPa. This value also shows a discrepancy with the expected value, and this can be explained as previously by a consideration of the shear and bending deflections.

CONCLUSIONS

In this study, we have observed the following:

- Both the normal stress and shear stress in bending depend strongly on the L/t ratio. This effect for shear failures is not easily predicted. For tensile failures, it is reasonably well predicted by the mechanics-of-materials theory.
- The shear fracture surface is at the interface or through the resin and not through the fibers.
- The interlaminar shear strength of the glass-fiber/epoxy-resin composite studied here, for $v_f = 0.65$, was around 50 MN/m^2.

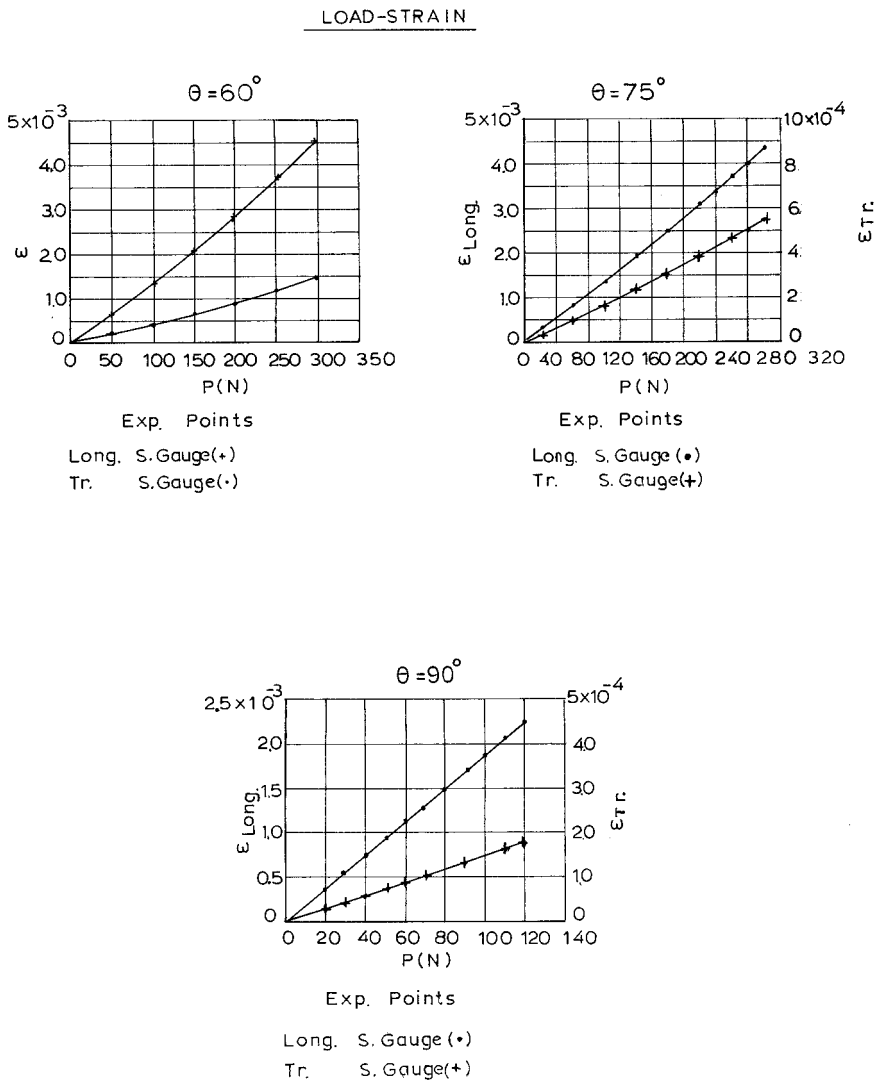

Figure 10 (*Continued from the previous page*)

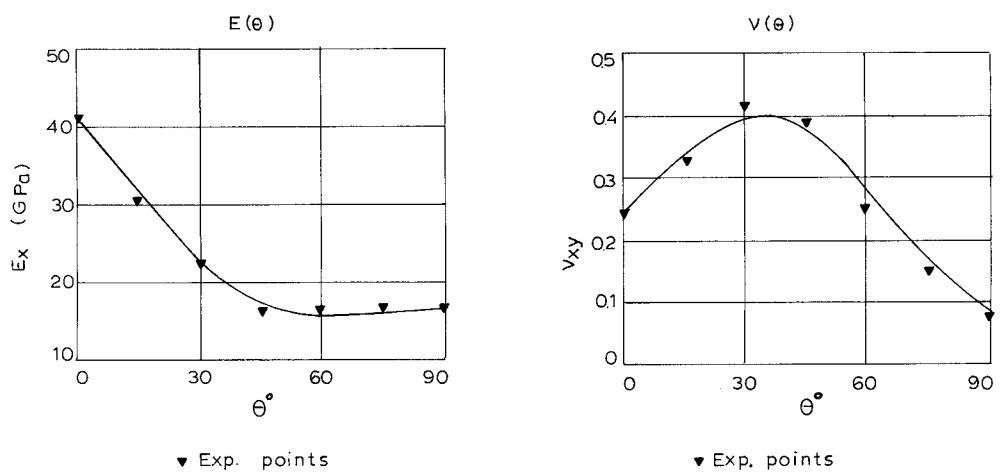

Figure 11 E_x and ν_{xy} versus θ.

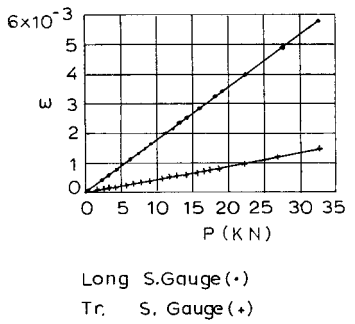

Figure 12 P–ε diagram obtained from a tension experiment at $\theta = 0°$.

The longitudinal value of E_b obtained experimentally showed a discrepancy from that expected and from the theoretical value; this can be attributed to the low value of L/t used, which did not give results too close to the tensile modulus also obtained experimentally.

The longitudinal value of E_b obtained from the deflection measurements also showed a significant discrepancy in comparison with the theoretical value.

APPENDIX

Strain transformation

$$\begin{Bmatrix} \varepsilon_x' \\ \varepsilon_y' \\ \dfrac{\gamma_{x'y'}}{2} \end{Bmatrix} = \begin{bmatrix} \cos^2\beta & \sin^2\beta & 2\sin\beta\cos\beta \\ \sin^2\beta & \cos^2\beta & -2\sin\beta\cos\beta \\ -\sin\beta\cos\beta & \sin\beta\cos\beta & \cos^2\beta - \sin^2\beta \end{bmatrix} \times \begin{Bmatrix} \varepsilon_x \\ \varepsilon_y \\ \dfrac{\gamma_{xy}}{2} \end{Bmatrix} \quad \text{(A.1)}$$

Influence of resin-rich layers

The E_t and E_b values of a laminate composite are supposed to be equal when it is composed of many identical layers. When there is some nonuniformity in the laminate, E_t and E_b will generally be different. In particular, a resin-rich layer on either or both of the surfaces can significantly affect E_b. Because E_t of the fiber is much greater than that of the resin, the direct contribution of the latter to the ability of a fabric-reinforced laminate to resist extensional and flexural deformation is usually small and can be neglected as a first approximation. Therefore, layers of resin on the outer surface(s) of a laminate have little effect on the deflection of a laterally loaded beam or plate. However, surface resin-rich layers do contribute to the laminate thickness used in computing E_t and E_b and can have a significant effect on the computed value of E_b.

Let us consider a laminated composite of total thickness t that has a resin-rich layer on either or both surfaces of combined thickness $t_{RRL} = \Delta t$. The thickness of the part of the composite containing the reinforcing fiber is

$$t_0 = t - t_{RRL} = t - \Delta t \quad \text{(A.2)}$$

As discussed previously, the contribution of the resin-rich layers to resisting deflection can be ignored, to a first approximation, unless they are extremely thick. That is, the lateral deformation of a laminate of thickness t having resin-rich layers of total thickness $t_{RRL} = \Delta t$ is almost the same as that of a laminate of thickness t_0 having no resin-rich layers under the same load. Similarly, the extensional deformations are the same.

Let us denote the extensional and bending moduli of a laminate of thickness t as E_t' and E_b', respectively. The corresponding properties of the laminate without resin-rich layer(s) are E_t and E_b, respectively. Deflections under load P being equated, the following relationship can be obtained from eq. (15):

$$E_b' = E_b\left(\frac{t_0}{t}\right)^3 \quad \text{(A.3)}$$

Similarly, by equating the strains under the same extensional load, we find that

$$E_t' = E_t\left(\frac{t_0}{t}\right) \quad \text{(A.4)}$$

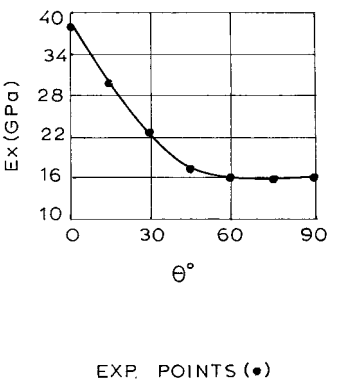

Figure 13 E_x versus θ according to deflection measurements.

With eq. (A.2), the previous equations can be rewritten, in terms of the total thickness and resin-rich-layer thickness, as follows:

$$E_b' = E_b\left(1 - \frac{\Delta t}{t}\right)^3 \cong E_t\left(1 - \frac{3\Delta t}{t}\right) \qquad (A.5)$$

$$E_t' \cong E_t\left(1 - \frac{\Delta t}{t}\right) \qquad (A.6)$$

The resin layer has a severe effect on the moduli, and this effect is much more important on E_b. The resistance to bending deformation of the two laminates is the same, but because of the extra resin, the modulus of the thicker one is lower. In other words, as eq. (12) shows, the deflection under a lateral load is governed by the beam flexural rigidities $E_b' t^3$ and $E_b t_0^3$, which are equal, although the moduli E_b' and E_b differ.

References

1. Chiao, C. C.; Moore, R. L.; Chiao, T. T. Composites 1977, 7, 161.
2. Christiansen, A. W.; Lilley, J.; Shortall, J. B. Fibre Sci Technol 1974, 7, 1.
3. Mullin, J. V.; Knoell, A. C. Mater Res Stand 1970, 10, 16.
4. Westwater, J. V. Am Soc Test Mater Proc 1949, 49, 1092.
5. Daniels, B. K.; Harakas, N. K.; Jackson, R. C. Fibre Sci Technol 1971, 3, 187.
6. Whitney, J. M.; Browning, C. E. Exp Mech 1985, 9, 294.
7. Berg, C. A.; Tirosh, J.; Israeli, M. Compos Mater: Test Des ASTM STP 1972, 497, 206.
8. Sandorff, P. E. J Compos Mater 1980, 14, 199.
9. ASTM D 2344-65T. Annu Book ASTM Stand 1965, Vol. 35.
10. Zweben, C.; Smith, W. S.; Wardle, M. W. Compos Mater: Test Des ASTM STP 1978, 674, 228.